

www.acsami.org Research Article

Highly Expandable Foam for Lithographic 3D Printing

David M. Wirth, Anna Jaquez, Sofia Gandarilla, Justin D. Hochberg, Derek C. Church, and Jonathan K. Pokorski*



Cite This: ACS Appl. Mater. Interfaces 2020, 12, 19033-19043



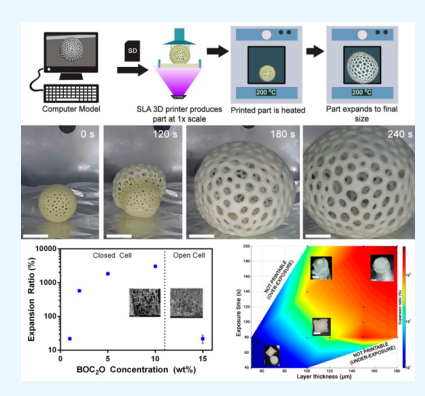
ACCESS

Metrics & More

Article Recommendations

Supporting Information

ABSTRACT: In modern manufacturing, it is a widely accepted limitation that the parts patterned by an additive or subtractive manufacturing process (i.e., a lathe, mill, or 3D printer) must be smaller than the machine itself that produced them. Once such parts are manufactured, they can be postprocessed, fastened together, welded, or adhesively bonded to form larger structures. We have developed a foaming prepolymer resin for lithographic additive manufacturing, which can be expanded after printing to produce parts up to 40× larger than their original volume. This allows for the fabrication of structures significantly larger than the build volume of the 3D printer that produced them. Complex geometries comprised of porous foams have implications in technologically demanding fields such as architecture, aerospace, energy, and biomedicine. This manuscript presents a comprehensive screening process for resin formulations, detailed analysis of printing parameters, and observed mechanical properties of the 3D-printed foams.



KEYWORDS: foams, 3D printing, additive manufacturing, digital light processing, high expansion

■ INTRODUCTION

Current methods of 3D printing (3DP) have enabled the fabrication of a wide variety of complex structures and geometries not possible through other forms of manufacturing. While additive manufacturing (AM) of polymers unlocks countless doors in terms of design and geometric freedom, these methods are generally limited by the repertoire of materials available to the specific processes and the size of printed parts to the confines of the 3D printer's build envelope. These material limitations become especially apparent when contrasted with mature polymer processing techniques such as extrusion or injection molding, which can be carried out using essentially any thermoplastic polymer. The limitation of part fabrication size is pervasive in nearly all additive manufacturing methods to date; it is this limitation that we aim to address in this work. Lab-scale 3DP of polymers is typically enabled by two technologies: fused deposition modeling (FDM) and stereolithography (SLA). FDM produces objects by extruding melted thermoplastics through a heated nozzle and is largely amenable to the materials used for melt processing techniques commonly employed by the polymer processing community. In contrast, SLA forms parts by selectively exposing light sensitive resins to patterns of light. The materials selection of SLA is significantly limited compared with FDM due to the chemistry needed to rapidly cure polymers with light. Thus, SLA has been traditionally restricted to materials that undergo photoinduced radical cross-linking of acrylates and acrylamides.^{1,2} Parts made with SLA are generally capable of much higher detail than FDM with minimal gradation between layers. However, the properties of SLA-produced parts are

limited, since commercial resins generally produce stiff, brittle, highly cross-linked parts. Efforts have been made to expand this selection of materials by incorporating novel resin chemistries, composites, or advanced methods of additive manufacturing, but such advances have traditionally relied on expensive equipment or specialized reagents.^{3–5} In short, there is a great need to expand the collection of materials available to SLA printing, and currently, there are no examples of highly expandable foams produced using this technique.

While 3DP offers a high degree of flexibility in the geometry of finished parts, the time required to print an object is proportional to its volume. Consequently, many commercial printers have small build volumes, forcing larger objects to be assembled from multiple separate prints. However, these limitations can be mitigated by developing resins that cure to form expanding polymeric foams, thus allowing one to print an object quickly at small scale and then expand it after printing to reach a larger finished scale. Perhaps the most famous example of a polymeric foam is expanded polystyrene 6 or Styrofoam. It has a broad range of applications due to its low cost, excellent insulating properties, ease of fabrication, and high expansion ratio $(20-90\times)$. However, polystyrene foam is not amenable to SLA printing due to its low cure rate and volatile blowing

Received: February 11, 2020 Accepted: March 27, 2020 Published: April 8, 2020





Table 1. List of Selected Resin Formulations Explored in the Current Study and Their Respective Cure Times^a

sample #	monomer	wt%	CL	wt%	PI	wt%	cure time (s)
A1	MMA	95	-	-	BAPO	5	720
A2	MMA	90	-	-	BAPO	10	540
A5	MMA	95	-	-	BAPO/TPO 1:1	5	660
A6	MMA	90	-	-	BAPO/TPO 1:1	10	205
A7	MMA	87.5	EGDMA	7.5	BAPO/TPO 1:1	5	520
A8	MMA	67.5	EGDMA	27.5	BAPO/TPO 1:1	5	110
A11	HEA	99	-	-	BAPO	1	10
A12	HEA	98	-	-	BAPO	2	5
A14	HEA	95	-	-	BAPO	5	15
A15	HEA	90	-	-	BAPO	10	20
A16	HEA	95	-	-	BAPO/TPO 1:1	5	10
A17	HEA	90	-	-	BAPO/TPO 1:1	10	15
A18	HEA	87.5	EGDMA	7.5	BAPO/TPO 1:1	5	15
A19	HEA	67.5	EGDMA	27.5	BAPO/TPO 1:1	5	20
A22	HEMA	98	-	-	BAPO	2	60
A23	HEMA	97	-	-	BAPO	3	50
A24	HEMA	95	-	-	BAPO	5	45
A25	HEMA	90	-	-	BAPO	10	60
A26	HEMA	95	-	-	BAPO/TPO 1:1	5	40
A27	HEMA	90	-	-	BAPO/TPO 1:1	10	55
A28	HEMA	87.5	EGDMA	7.5	BAPO/TPO 1:1	5	30
A29	HEMA	67.5	EGDMA	27.5	BAPO/TPO 1:1	5	20

"Cure time was evaluated with a 340 μ W/cm², 405 nm light source via the method of Figure 1A. A comprehensive list of compositions can be found in Tables S1 and S2. List of acronyms used in this table: phenylbis(2,4,6-trimethylbenzoyl)phosphine oxide (BAPO), diphenyl(2,4,6-trimethylbenzoyl)phosphine oxide (TPO), ethylene glycol dimethacrylate (EGDMA), methyl methacrylate (MMA), hydroxyethyl acrylate (HEA), and hydroxyethyl methacrylate (HEMA).

agents (such as pentane), which would evaporate from the resin bath during long prints. Researchers have attempted to solve this problem by creating 3D printable foam materials using direct ink writing 8,9 or FDM, $^{10-12}$ but the resultant parts generally have low expansion ratios or poor resolution in comparison to SLA parts. Many of these methods rely on the patterning of a cured polymer with a dissolvable component (such as salt⁹ or sugar¹³) and submerging the structure in water after the print is complete, leaving a porous, open-celled sponge. While these methods are promising for a variety of applications, particularly in biomedicine, many are ill suited to a broad range of applications due to their open-cell nature, negligible expansion, ¹⁰ and/or low mechanical strength (typically under a 0.1 MPa modulus). ^{9,13} Recently, an inkjet 3DP formulation using a hydrazine-based blowing agent, 4,4'oxybis(N'-benzoylbenzenesulfonohydrazide), demonstrated up to 44% volumetric expansion using a modified PolyJet system. 14 While this initial work is promising, it relies on a specialized system and requires a pre-expansion prior to fully curing the part, making the process unsuitable for SLA systems.

In our work, we aimed to use a widely available mask stereolithography (MSLA) system, the Anycubic Photon, which costs under \$300 and does not rely on sensitive optics. While this printer is highly accessible to researchers, it is only able to produce a light intensity less than 1 mW/cm². Based on the available literature and the nature of the MSLA process, we propose the following conditions are necessary to create a foamable resin for MSLA printers

- (1) The prepolymer resin must cure quickly at light intensities under $1~{\rm mW/cm^2}$ to allow for practical print times.
- (2) The decomposition point of the blowing agent must be above the glass transition (T_g) and below the melting

- $(T_{\rm m})$ or decomposition temperature $(T_{\rm d})$ of the cured polymer to allow for deformation and gas trapping but not melting or decomposition of the printed object during expansion.
- (3) The blowing agent must be soluble in the neat monomer to prevent precipitation during the print in order to ensure homogeneous expansion of the printed part.
- (4) The prepolymer resin must contain a low concentration of cross-linking species. Cross-links increase the glass transition temperature of the printed object as well as reduce the free volume of the polymer, leading to reduced expansion of foams.

Herein, we describe a resin formulation that can be printed in an unexpanded state and controllably expanded to create structures significantly larger than their printed size. We present a systematic evaluation of resin components including monomers, blowing agents (BA), and photoinitiators (PI). Finally, we present an evaluation of 3D print parameters to enable controllable foaming, analysis of the mechanical properties of several foam variants, and demonstrations for potential applications of the technology (available in the supplemental videos).

■ RESULTS AND DISCUSSION

Optimization of Resin Formulation and Cure Time.

Monomer Composition. In order to develop a resin, our first endeavor was to determine a monomer that was suitable for 3D printing and characterize its layer curing time. Three potential monomers were explored for a foaming resin: methyl methacrylate (MMA), 2-hydroxyethyl acrylate (HEA), and 2-hydroxyethyl methacrylate (HEMA) (Table 1). Rather than doing full-scale prints for each composition, the cure time for each formulation was evaluated by placing a 20 µL droplet of

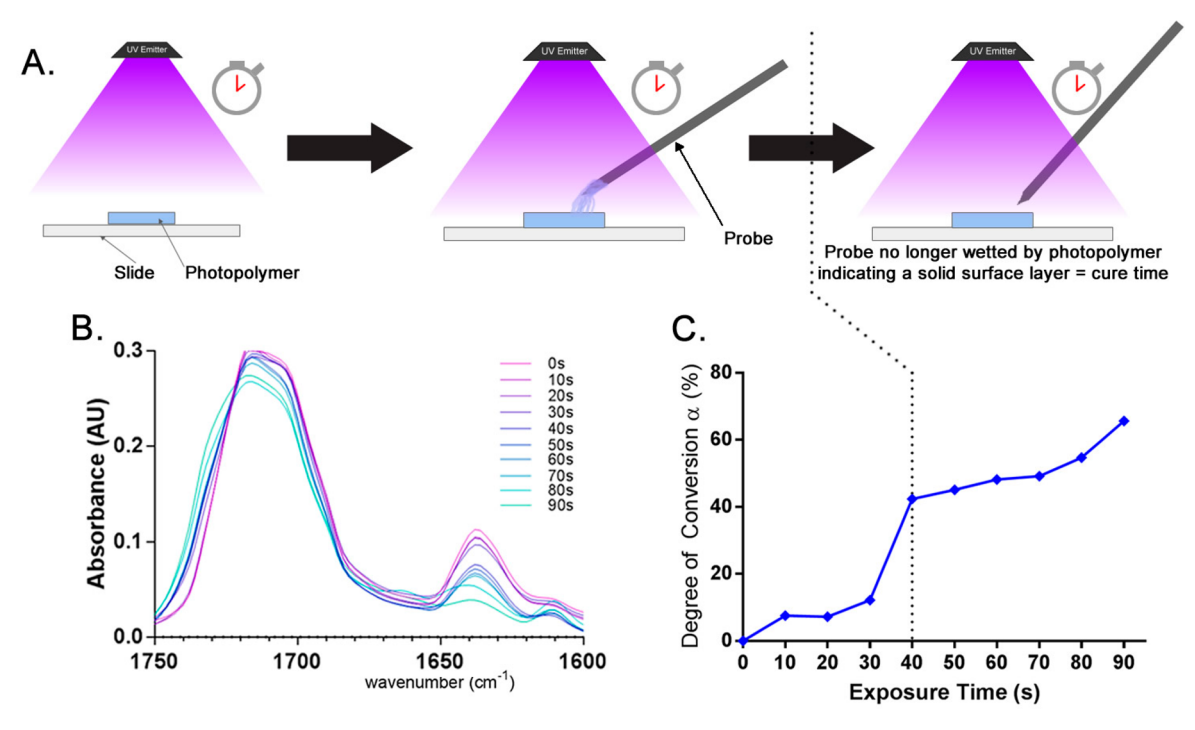


Figure 1. (A) Procedure used for experimentally determining cure time, which correlated to FTIR data, of a variety of photopolymer resins. (B) Selected region of FTIR absorbance spectra corresponding with eq 1 for a pHEMA photopolymer with 5 wt % BAPO/TPO (in a 1:1 molar ratio). (C) Calculated degree of conversion of (B) as a function of exposure time (s) under a 0.34 mW/cm² light source at 405 nm. Raw FTIR data and photographs of cured polymers can be found in Supplemental Figure S10.

each resin composition on a glass slide and exposing them to a 340 μ W/cm², 405 nm light source while periodically inserting a metal probe into the liquid resin until the probe was no longer wetted by the polymer sample. This provided a reliable indication of the minimum exposure time for viable 3D printing layers of new resin formulations and accelerated our ability to test compositions (Figure 1A,E).

Despite MMA's widespread use in commercial resins, it is commonly augmented by a large proportion of cross-linker (CL) and oligomer species, without which MMA would be impractical due to its slow cure rate. 15 Our results further verify this, and even at high concentrations of the cross-linker ethylene glycol dimethacrylate (EGDMA), the cure time was in excess of 100 s (entry A8, Table 1). Furthermore, the thermal window between $T_{\rm g}$ (85 16 –102 17 °C) and $T_{\rm m}$ (160 °C16) was fairly narrow, making appropriate pairing with a blowing agent difficult. Other widely used monomers that are cured by radical polymerization, such as urethane acrylate oligomers, tripropylene glycol diacrylate, bisphenol A-glycidyl methacrylate, and tetraacrylates, 15 were not explored in this work, because they would form a tightly cross-linked network in a finished part. Cross-linked polymers tend to decompose rather than soften or melt; thus, they are less amenable to foam expansion. Consequently, we aimed to minimize the use of cross-linking species in our resin formulations and discarded MMA for future development.

Of the monomers tested, HEMA and HEA were promising candidates due to their rapid cure times and current use in 3DP scientific literature. ^{18,19} It is known that these monomers contain small amounts of cross-linking species that helped to accelerate curing but were present in sufficiently low concentrations to enable expansion (1.72 mol % in HEA vs 0.18 mol % in HEMA) (Figure S8). The cure rate of HEA was roughly 1 order of magnitude faster than that of HEMA.

Additional cross-linking components were tested to improve cure time; however, the cure rate was negligibly enhanced (entries A18, 19, 28, 29, Table 1). HEA compositions cured quickly, but the mechanical and gas retention properties of the final pHEA polymer were poor in comparison to pHEMA (see section on Development of Foaming Resin Formulation). While pHEMA is mechanically rigid even without the use of additional cross-linkers, pHEA is mechanically pliable and allows gas to escape during expansion (Table 2). The very low glass transition temperature ($T_{\rm g}$ < 0 °C) of pHEA is poorly suited for its use in expanding foams, which must hold their shape during expansion. HEMA was chosen as the most

Table 2. Composition of Blowing Agents Explored in the Current Study a

blowing agent	thermolysis temperature (°C)	benefits	drawbacks
BOC ₂ O	196-22017	solubility , high gas production	toxicity
ADC	$150-190^a (205-215)^{22}$	high gas production	insoluble in all monomers
TSH	120-130 ²²	low decomposition temperature	low gas production, poor solubility
NaHCO ₃	160 ²³	nontoxic, inexpensive, high gas production	insoluble, low gas production
H ₂ O	100 ^b	safe, miscible with monomers, high gas production	plasticizer for HEMA and HEA, uneven expansion, large cell size of foams
EA	77 ^b	safe, miscible with monomers, high gas production	uneven expansion, large cell size, volatility

"When used with urea and ZnO as activators. b Boils rather than decomposes.

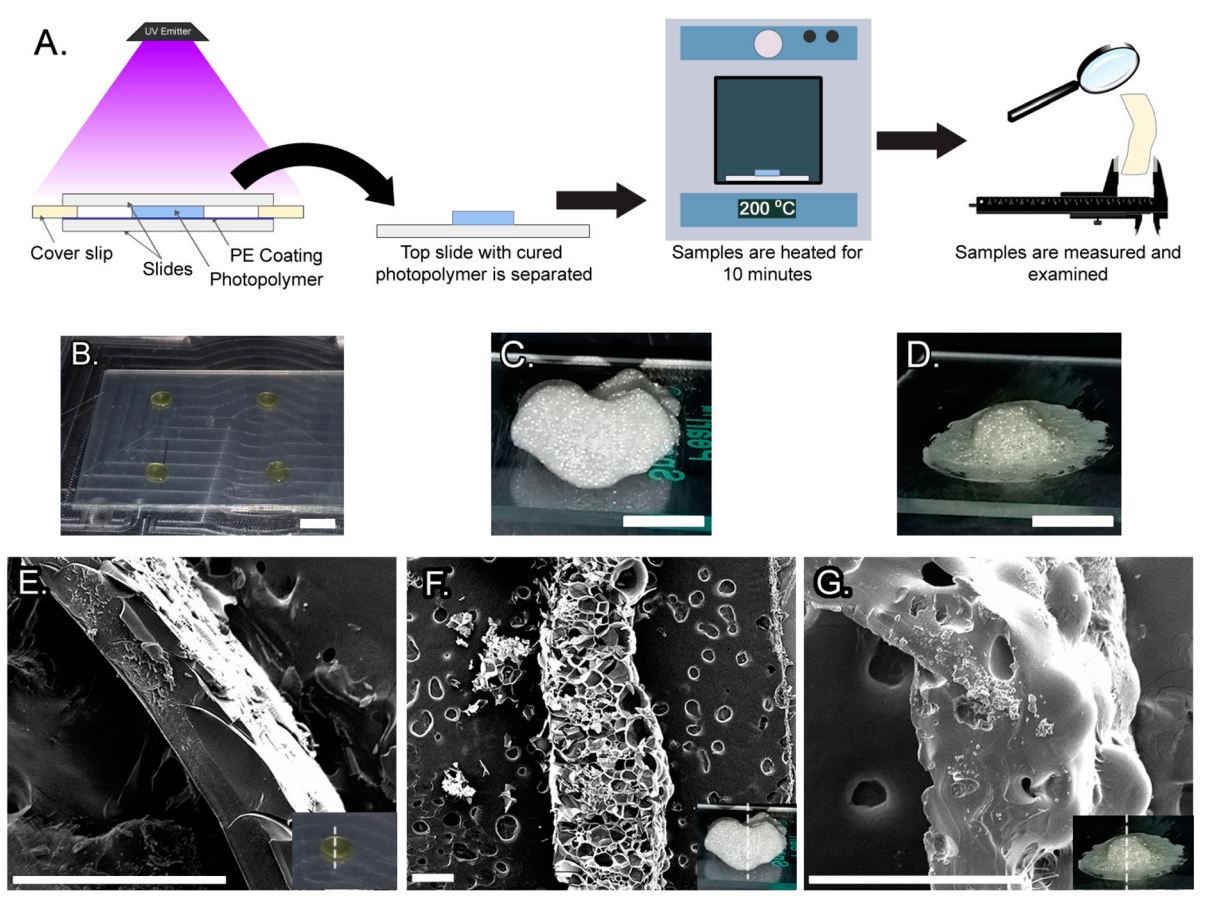


Figure 2. (A) Procedure used for experimentally determining the expansion ratio of small samples of foaming polymer. (B) Photograph of unexpanded polymer samples prior to heating. (C) Photograph of pHEMA polymer sample containing 10 wt % BOC₂O after heating. (D) Photograph of pHEA polymer sample containing 10 wt % BOC₂O after heating. (E) Cross-sectional micrograph of unexpanded polyHEMA, 10 wt % Boc₂O under SEM. (F) Cross-sectional micrograph of C) under SEM. (G) Cross-sectional micrograph of D under SEM ((B-D): scale bars 5 mm, (E-G): scale bars 500 μ m). Note: the circular pores in the backgrounds of (F) and (G) are artifacts in the conductive carbon tape adhesive rather than the foamed polymer.

promising monomer in initial screenings due to its stability in ambient conditions, reasonable cure time, favorable mechanical properties, glass transition temperature above room temperature ($T_{\rm g}=70^{20}-82^{17}$ °C), and a high decomposition temperature ($T_{\rm d}=230-293^{17}$ °C).

In order to correlate these empirical findings to theoretical models in the literature, 21 FTIR spectroscopic analysis was carried out on our most promising resin, HEMA, by determining the disappearance of the band at 1636 cm⁻¹, when compared to an internal control at 1718 cm⁻¹, using eq 1 to correlate degree of conversion (α) with light dosage at a given time (Figure 1B–D).

$$\alpha = 100* \left\{ 1 - \frac{\left[(A_{1636\text{cm}^{-1}}) / A_{1718\text{cm}^{-1}} \right]_t}{\left[(A_{1636\text{cm}^{-1}}) / A_{1718\text{cm}^{-1}} \right]_{t=0}} \right\}$$
 (1)

FTIR spectra were taken of HEMA with 5 wt % photoinitiator with samples taken at 10 s time points (sample A26, Table 1). The absorbance values in eq 1 correspond to absorption peaks of C=O and C=C bonds at 1718 and 1636 cm⁻¹, respectively. While the FTIR analysis is not strictly necessary for evaluating the potential resins for 3D printing, it was conducted to verify that our results correspond well to theoretical models. Our experimental data agrees with the theoretical predictions in the literature that once a "threshold" dose of light is delivered to a volume of resin, its degree of conversion undergoes a sharp

transition.²¹ This threshold also corresponds to the point at which the resin turned from a sticky gel into a solid. The time required to achieve this threshold dose at a given light intensity we define as the "cure time", which is the minimum layer exposure time for which 3D printing of the material is viable.

Optimization of Photoinitiator. Following identification of suitable monomers, a more comprehensive screen took place, which considered photoinitiator species and concentration and the pairing with an appropriate blowing agent (Table S1). Two PIs and combinations thereof were tested for their amenability for curing in a traditional 405 nm SLA system (Tables 1 and S1). Phenylbis(2,4,6-trimethylbenzoyl)phosphine oxide (BAPO) and diphenyl(2,4,6-trimethylbenzoyl)phosphine oxide (TPO) both produced a rapid cure at 405 nm. BAPO/TPO in a 1:1 molar ratio was especially versatile and produced the best cure performance for many of the monomers tested, including HEMA. Formulations containing HEMA cured fastest when using high concentrations of PI at 5 wt %, whereas 2-hydroxyethyl acrylate (HEA) formulations provided the most rapid curing at low concentrations of PI between 1 and 2 wt %.

Development of Foaming Resin Formulation. Determining a synergistic combination of blowing agent (BA) and monomer was perhaps the most challenging aspect of resin development. After HEMA was selected as a monomer, it was

Table 3. List of Selected Relevant Foaming Resin Formulations Discussed in the Current Study, along with Their Respective Cure Times and Expansion Ratios^a

sample #	monomer	wt %	CL	wt %	PI	wt %	BA	wt %	cure time (s)	exp. ratio
C1	HEMA	93	-	-	BAPO/TPO 1:1	5	BOC ₂ O	2	40	50%
C2	HEMA	90	-	-	BAPO/TPO 1:1	5	BOC_2O	5	40	250%
C3	HEMA	85	-	-	BAPO/TPO 1:1	5	BOC_2O	10	40	750%
C4	HEA	85	-	-	BAPO/TPO 1:1	5	BOC_2O	10	40	100%
C8	HEMA	84	EGDMA	1	BAPO/TPO 1:1	5	BOC_2O	10	40	60%
C11	HEMA	84	PEGDA575	1	BAPO/TPO 1:1	5	BOC ₂ O	10	40	200%

"Cure time was evaluated with a 340 μ W/cm², 405 nm light source via the method of Figure 1A. The expansion ratio was evaluated via the method of Figure 2A and expressed as the ratio between the initial and final thicknesses of films before and after heating at 200 °C for 10 min where 0% indicated no change in thickness. A more comprehensive list of compositions explored can be found in Tables S2—S4. List of acronyms used in this table: phenylbis(2,4,6-trimethylbenzoyl)phosphine oxide (BAPO), diphenyl(2,4,6-trimethylbenzoyl)phosphine oxide (TPO), ethylene glycol dimethacrylate (EGDMA), poly(ethylene glycol) diacrylate $M_n = 575$ (PEGDA575), di-tert-butyl dicarbonate (BOC₂O), hydroxyethyl acrylate (HEA), and hydroxyethyl methacrylate (HEMA).

necessary to select a blowing agent with a decomposition temperature below that of pHEMA ($T_{\rm d}=230~^{\circ}{\rm C}$), but above that of HEMA's glass transition ($T_{\rm g}=70-82~^{\circ}{\rm C}$), while maintaining low volatility to avoid evaporation over the course of a multihour print. Table 2 summarizes the advantages and disadvantages of a number of common blowing agents employed in industry or in literature including di-tert-butyl dicarbonate (BOC₂O), azodicarbonamide (ADC), p-toluene-sulfonhydrazide (TSH), sodium bicarbonate (NaHCO₃), water (H₂O), and ethyl acetate (EA).

Many of these blowing agents are largely insoluble or difficult to stabilize as emulsions in HEMA (see results in Table S2). Slow precipitation of undissolved blowing agent led to an inhomogeneity of prints and uneven expansion of the finished parts. While ADC and NaHCO3 both produce copious amounts of gas, especially in the presence of activators (such as urea, citric acid, and zinc oxide), they were the least soluble in all monomers found suitable for printing. TSH had better solubility but also produced the lowest volume of gas and proved unreliable as a blowing agent. Solvent-based blowing agents such as hexane, toluene, ethyl acetate, or pentane exhibited high volatility and would evaporate from the resin bath prints, rendering them ill-suited for application in SLA 3D printing. Water was explored as a blowing agent, but due to its activity as a plasticizer in pHEMA, 26 it resulted in foams with very large cell sizes and/or foams that were unable to contain the expansion of resultant steam. Lowering the concentration of water resulted in insufficient and uneven expansion of the final foams.

Due to our dissatisfaction with traditional blowing agents, we sought to use a nontraditional agent that is soluble in organic solvents, decomposes at low temperatures, and yields a high molar volume of gas upon decomposition. BOC₂O is soluble in many organic liquids (including neat HEMA, HEA, and MMA), thermolyzes at a low temperature (into 4 mol of gaseous products), and has recently been the subject of study both as an epoxy blowing agent²⁷ and also as a conjugated moiety on both poly(4-(tert-butoxycarbonyloxy)-styrene) and poly(2-(tert-butoxy-carbonyloxy)ethyl methacrylate),^{17,28} but to our knowledge, such polymers have yet to be employed in a 3D printing capacity. BOC₂O is not commonly employed as a polymer blowing agent due to its reactivity and reports of its toxicity in gaseous form. Because of these concerns, we evaluated the chemical compatibility for use in this application.

NMR analysis (Figures S1 and S2) revealed that BOC₂O is unreactive toward the HEMA monomer and that the solution

is chemically stable when mixed for up to 1 week. Thermogravimetric analysis (TGA) (Figure S6) demonstrated a two-step decomposition of the pHEMA/BOC2O polymer with a first phase of weight loss occurring between 100 and 150 °C and the second phase above 160 °C consistent with the decomposition temperature of BOC₂O. ^{17,28,29} We attempted to assess the risks of thermolyzing large quantities of BOC₂O by characterizing the gaseous effluents of the resultant foams to determine if any potentially toxic compounds were generated. Based on the results of the TGA, thermal expansion was conducted at a temperature of 200 °C to ensure complete decomposition of BOC₂O. GC-MS headspace analysis (Figure S7) found no detectable BOC₂O residue in samples of BOC₂O in pHEMA after heating to 200 °C for 10 min. The effluents consisted of only gaseous thermolysis products (tbutanol, CO2, and isobutylene), and no appreciable vaporized BOC₂O was released during expansion. Nevertheless, due to the reported toxicity of BOC₂O, we erred on the side of caution and conducted all large-scale tests of this material in a vacuum oven connected to a gas scrubbing system, which was repeatedly flushed before opening. An alternate approach would be to conduct expansion in a vacuum oven vented through an in-line filter of NaOH pellets or to conduct expansion in a fume hood.

We attempted to optimize and quantify the expansion ratio of small samples of foaming polymer mixtures using the test setup of Figure 2A: 20 µL droplets of liquid resin with blowing agent were placed between two glass slides, one of which was coated with a nonstick polyethylene film and separated by two 120 μ m thick glass coverslips (Figure 2B). After exposure to light, the samples cured and were transferred to an oven preheated to 200 °C, (Figure 2C,D), removed from the slide, and measured to determine their expansion ratio. Samples of HEMA and HEA were also imaged under SEM (Figures 2E-G) to demonstrate foam morphology. Tests with BOC₂O as a blowing agent are documented in Tables 3 and S3 and regularly demonstrated expansion ratios between 50 and 750%. Approximate foam cell size (measured via SEM using a random selection of five cells) correlated inversely with BOC₂O content and ranged from 75 to 1200 μ m. A subset of tests conducted with alternate blowing agents are documented in Table S2 and generally achieved expansion ratios between 0 and 200% with one formulation containing ADC achieving up to 400%; however, poor mechanical properties or inhomogeneity of the materials led us to proceed with BOC₂O as a blowing agent. Figure S5 demonstrates the

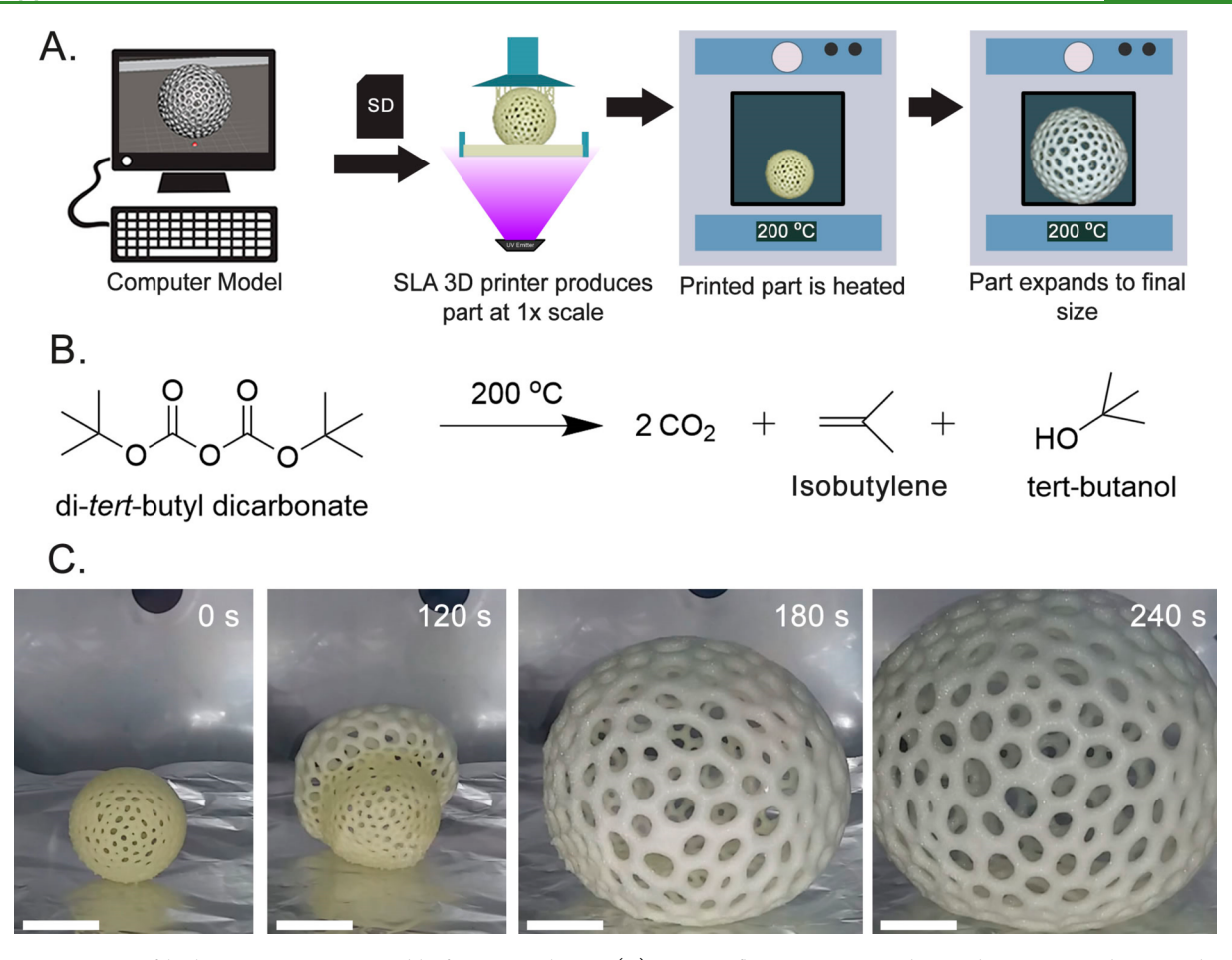


Figure 3. Overview of high expansion 3D printable foaming polymer. (A) Process flow: structure is designed on CAD and exported to STL. Structure is printed at reduced scale and then heated at 200 $^{\circ}$ C and expanded to final size. (B) Decomposition of BOC₂O, which serves as the blowing agent for expansion. A total of 4 moles of gas are produced per mole of solid. (C) Photographic time frame images taken of a Voronoi sphere showing high expansion ratio of printed parts over the course of a 4 min expansion (scale bars 25 mm).

difference in expansion ratio and uniformity between selected compositions containing BOC₂O and other blowing agents.

Foams using HEA as a monomer (Figure 2D) cured quickly but had low stiffness and could not trap gases as well as HEMA-based foams (Figure 2C), thereby resulting in a lower expansion ratio. Mixtures of pHEMA using BOC_2O as a blowing agent yielded the best performance out of all combinations tested and were thus were selected as the baseline resins for full-scale prints.

Characterization of the Presence and Impact of Added Cross-Linkers. In order to create a polymeric foam upon heating an unconfined blend of polymer and blowing agent, it was necessary to select a blowing agent with a decomposition temperature above that of the glass transition temperature of the polymer. It is well documented that the addition of a cross-linker dramatically increases and eventually altogether eliminates the glass transition temperature of a polymer.³⁰ The addition of cross-linkers such as EGDMA or poly(ethylene glycol) diacrylate $M_n = 575$ (PEGDA575) modestly enhanced the cure rate of formulations to which they were added, but predictably reduced the expansion of resulting foams based on the final amount of cross-linker in the formulation (Tables 3 and S4). This may be beneficial as for some applications, as it offers another variable to tune the expansion ratio of foams.

When cross-linkers were added to formulations consisting of 10 wt % BOC₂O in a solution of HEMA (Table 3, entry C3), the addition of 0.5 wt % cross-linker decreased foam expansion by roughly a factor of 2, and the addition of 1.0 wt % crosslinker decreased foam expansion by a factor of 4–12. Addition of EGDMA resulted in a more dramatic reduction of foam expansion than addition of PEGDA575. We hypothesize that the increased glass transition temperature and rigidity of crosslinked polymers increases the viscosity of the polymer when heated to the blowing agent's decomposition temperature, thereby resulting in less deformation of the polymer as gas is released, causing higher pressure gas to build up within the softened polymer rather than expanding. Therefore, the best expansion relied on neat monomers with minimal cross-linking activity and little to no added cross-linking species. HEA has been shown in the literature to contain up to 10 wt % of intrinsic cross-linking species; 19 the concentration was less than 2 wt % in our tests via GC-MS (Figure S8). Furthermore, we found such intrinsic cross-linking species to comprise 0.18 wt % in HEMA samples.

3D Printing of Expandable HEMA/BOC₂O Resin. The general process flow for the SLA 3D printing of highly expandable polymeric foams consists of modeling an object in computer aided drafting software (CAD), which is then sliced into layers using software tools (Figure 3A). These digital slices are saved on a storage card or stick (SD), and the 3D

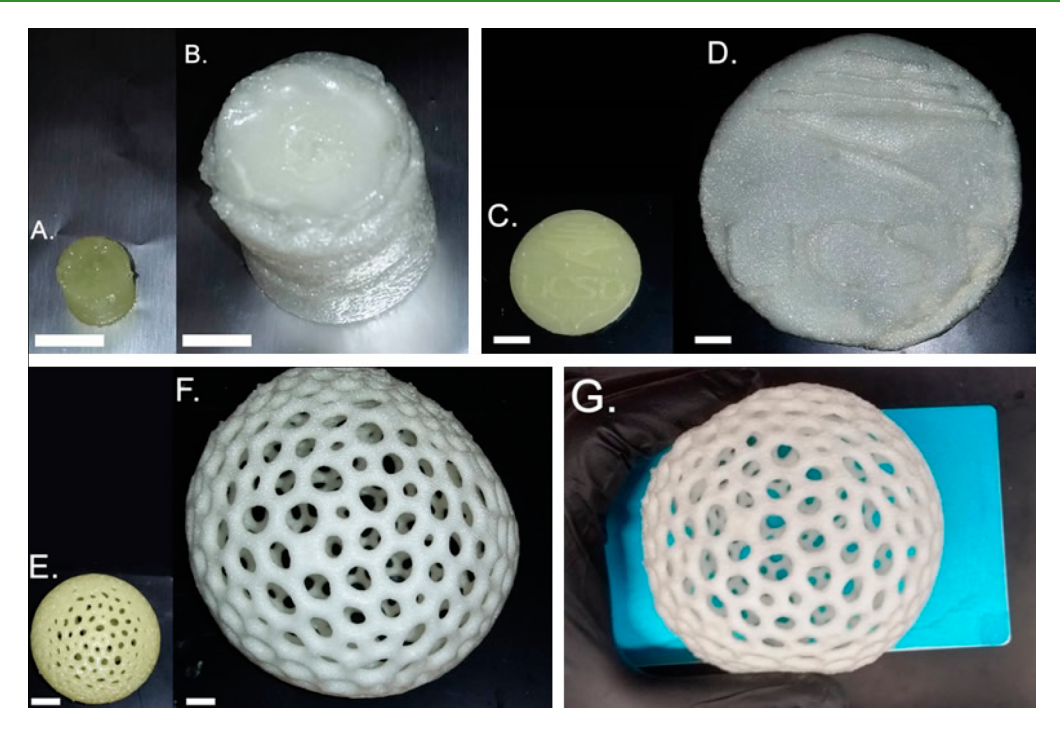


Figure 4. Samples shown before and after expansion at 200 °C for 10 min. Both samples were 3D-printed with 65 s of exposure at 0.18 mm layer height from the same bath of resin composed of 10 wt % BOC_2O , 2.5 wt % TPO, and 2.5 wt % BAPO in HEMA. (A) Cylinder (10×10 mm) before and (B) after expansion, (C) 35 mm diameter "puck" before and (D) after expansion, (E) 43 mm Voronoi sphere before and (F) after expansion. G) Demonstration of the size of the Voronoi sphere relative to the Anycubic build plate, demonstrating production of objects larger than the printer's build volume. All scale bars 10 mm.

printer projects patterns of light in the shape of the digital slices sequentially to produce a finished object at 1× scale. The part is then cleaned and supports are removed, and the part is heated at 200 °C for 10 min, causing the BOC₂O to thermolyze into 4 mol of gaseous products (Figure 3B). This expands the printed part to its final size by creating gas bubbles within the thermoplastic printed polymer part. The size of these gas bubbles and thus the ratio of expansion can be controlled digitally (by varying the height of printed layers) or chemically (by varying the BOC₂O content of the resin). Figure 3C shows the expansion process at a series of time points over the course of 4 min.

This process is extremely versatile, allowing a user to produce a wide variety of sample geometries including simple shapes such as cylinders (Figure 4A,B) and disks (Figure 4C,D) as well as more complex shapes such as Voronoi (Figure 4E,F) structures or cubic lattices (Figure S4). Importantly, this method demonstrates the capacity to produce objects larger than the build plate of the printer (Figure 4G). All samples in Figure 4 were produced with resin consisting of 10 wt % BOC₂O and 5 wt % of a 1:1 molar ratio of BAPO/TPO in HEMA. It was observed that objects with solid infill tended to split open or expand unevenly, and the most promising results were had with lattices, Voronoi meshes, or hollow structures. It was also found that thin structures or thin portions of structures with one or more dimensions less than 2 mm tended to expand unevenly. We hypothesize that this behavior is due to the inability of such thin segments to effectively trap gases when the polymer is heated above its $T_{\rm g}$. Conversely, structures with thickness exceeding 10 mm in all dimensions tended to overexpand, showing splitting behavior and uneven expansion. We hypothesize that this behavior is due to gas buildup within the center of the structure leading to a high rate

of expansion; this high rate of expansion causes the outer layers to undergo a ductile to brittle transition due to the non-Newtonian nature of polymers under tensile loading.³¹ Thin parts (such as disks or flat plates) tended to contort and flex during expansion but most eventually righted themselves to roughly their original shape once all portions of the polymer had fully expanded. Examples of this behavior can be observed in the supplemental videos.

We found that 3D-printed structures with 10 wt % BOC₂O tended to expand to a final size between 1 and 40× of their original volume (1–3.5× of original width) as shown in Figures 4 and 5. For the remainder of this work, we defined a volumetric expansion ratio parameter as eq 2, where $\rho_{\rm i}$ is the initial density of the unexpanded polymer, and $\rho_{\rm f}$ is the final density of the foam after expansion.

expansion ratio =
$$100*\left(\frac{\rho_{\rm i}}{\rho_{\rm f}}-1\right)$$
 (2)

Expansion of most printed parts occurred after 3–5 min of heating and parts expanded to their full size within 10 min, nucleating at a single or a few points simultaneously. Conversion followed an expansion front until the entire part had been converted to foam. The reproducibility of expansion ratios of 3D-printed parts was remarkably consistent, with triplicate samples usually falling within $\pm 15\%$ of the mean value (by average normalized standard deviation). To date, the largest volumetric expansion ratio of layer-by-layer structures was demonstrated by Wagner et al. (74% by density/bounding volume). The current work demonstrates expansions of roughly 4000% by density, comparable with the expansion of commercial Styrofoam. 32

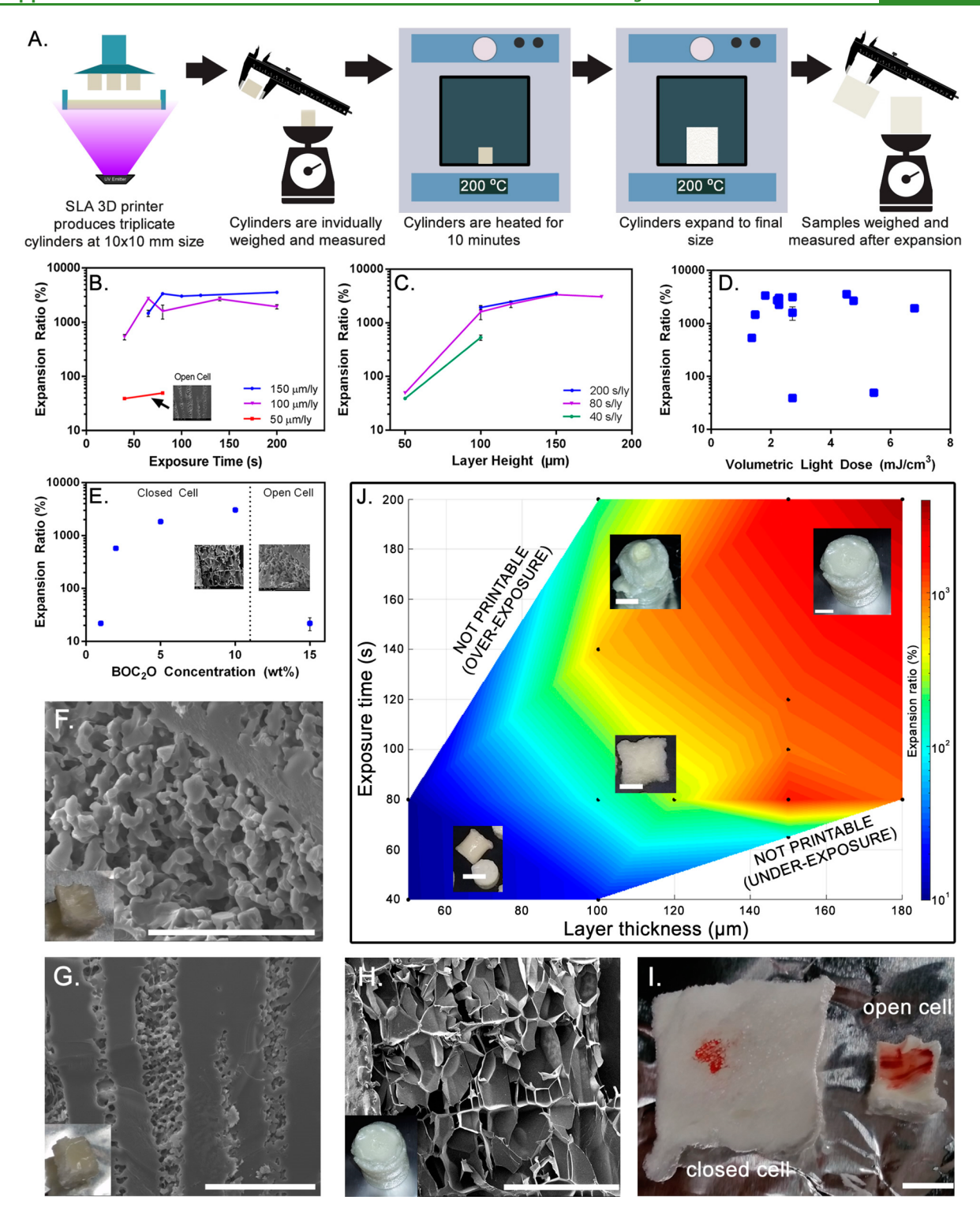


Figure 5. (A) Diagram of the process used to evaluate the expansion ratio of various print parameters, the results of which are shown below. (B) Expansion ratio vs exposure time, (C) expansion ratio vs layer height, (D) expansion ratio vs volumetric light dose, and (E) expansion ratio vs blowing agent concentration. SEM micrographs of selected samples: (F) 15 wt % BOC₂O open-cell foam, (G) 10 wt % BOC₂O open-cell foam, (H) 10 wt % BOC₂O closed-cell foam. (I) Effect of red food dye on open- and closed-cell foams, (J) 2D contour plot of exposure time and layer thickness vs expansion ratio. Scale bars: (F,G) 0.1 mm, (H) 1 mm, (I) 10 mm, (J) 10 mm.

Digital Control of Expansion Ratio and Cellular Structure. In order to examine the effect of print parameters, such as layer height and layer exposure time, on the expansion of foaming structures, cylinders $(10 \times 10 \text{ mm})$ were printed in triplicate from a single bath of resin (Figure 5A, also see Figure S11 for print images and model design). We found that both

layer thickness and light exposure time effected not only the *expansion* of foams after printing but also the *cellular structure* of foams (open cell vs closed cell). Print parameters were studied to quantitatively determine the effect on expandable pHEMA/BOC₂O foams (Figures 5 and S10).

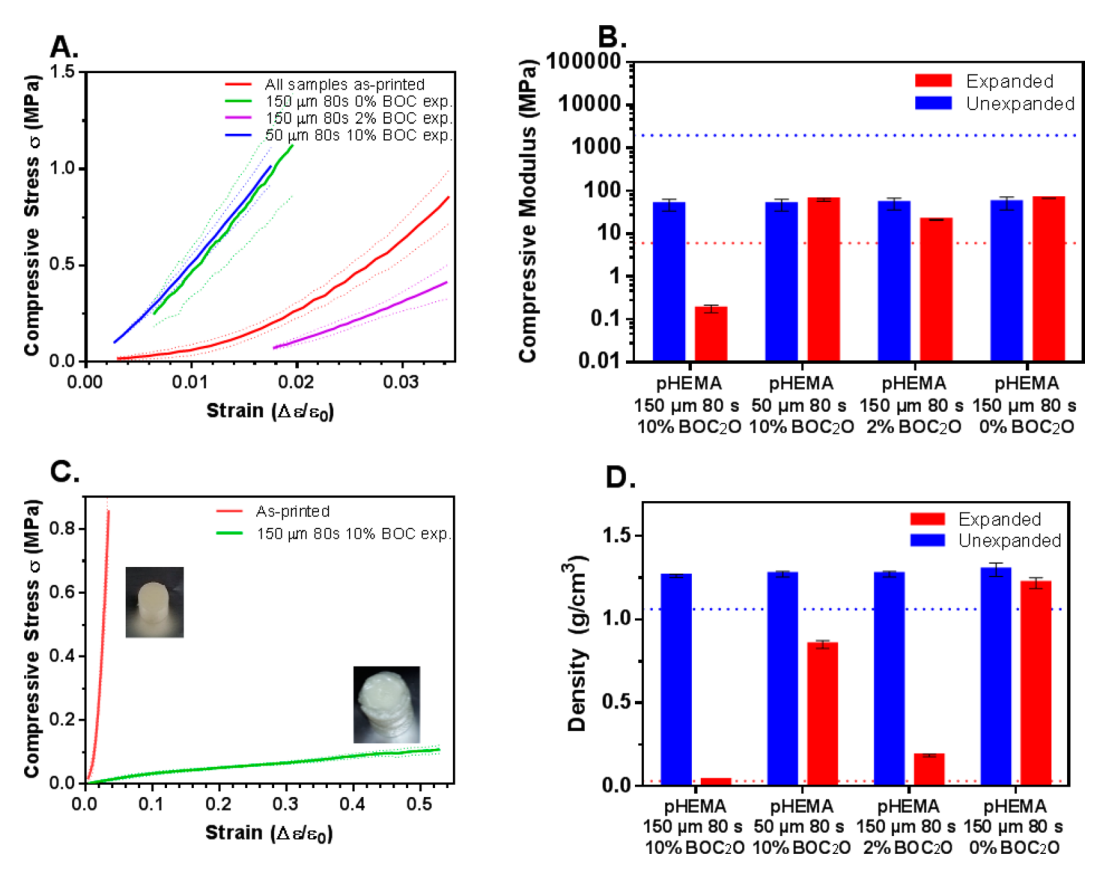


Figure 6. (A–D) Mechanical compressive analysis and summary of physical properties of foam polymer samples prepared from a solution of 2.5 wt % TPO and 2.5 wt % BAPO in HEMA with varying concentrations of BOC₂O and varying layer heights comparing mechanical properties before and after heating compared with those of commercial Styrofoam (shown as dotted lines on B and D). (A) Mechanical stress/strain behavior of samples with low expansion ratios before and after expansion. (B) Summary of compressive moduli of samples before and after expansion. (C) Mechanical behavior of a 150 μ m/80 s (high expansion ratio) sample before and after expansion, highlighting the large change in modulus. Data sets are shown on different axes for sake of clarity. (D) Summary of changes in density before and after expansion. Studies were carried out in triplicate, and dotted lines show standard error margin between sample runs.

When print parameters were varied between tests, it was found that the expansion ratio was most heavily dependent on layer thickness (Figure 5B,C), and there was no correlation between volumetric light dosage and expansion ratio (Figure 5D). Several samples were printed with a 150 μ m layer thickness and 80 s exposure time in HEMA resin with varying concentrations of BOC₂O to determine the effect of BOC₂O concentration on expansion ratio (Figure 5E). The results were surprising: as expected, increasing the concentration of BOC₂O up to 10 wt % increased the expansion ratio, but increasing the concentration over 10 wt % resulted in a dramatic drop in expansion ratio and a change in structure to open-cell foams (Figure 5F). Interestingly, a similar effect was observed when foams were printed with a layer thickness below 100 μ m, where the resultant foams adopted an open-cell structure and showed negligible expansion (Figure 5B,G). These results contrasted with the closed-cell structure of all other highly expanded samples (Figure 5H). The open- and closed-cell foams were compared qualitatively by cutting them open and adding a drop of red food dye to the surface (Figure 5I). Due to the hydrophilic nature of pHEMA, the water-based food dye penetrated into the pores of the open-cell foam; in contrast, the dye only stained the surface of the closed-cell samples. Figure 5J summarizes our results from over 50 samples printed from a resin bath containing 10 wt % BOC₂O and printed at varying layer thicknesses and exposure times. It

was necessary to maintain the layer exposure time within a window for a given layer thickness to prevent over- or underexposure of the print (both cases leading to print failure as shown in Figure S3), but within this window, exposure time had a negligible correlation with expansion ratio (Figure 5B). Below a 100 μ m layer thickness, the foams formed open-cell structures, and above a 100 μ m layer thickness, the foams formed closed-cell structures and trapped gases effectively, expanding up to 40× (4000%) by volume at layer thicknesses of 150–180 μ m. A general trend was observed that longer exposure times at higher layer thicknesses produced higher expansion ratios; but in making the layers thicker, one sacrifices print resolution, and in making exposure times longer, one greatly extends the print time.

Mechanical Testing of 3D-Printed Foams. Compression testing was conducted on samples of foamed polymer as well as the virgin polymer. All samples were triplicates of printed cylinders with a diameter of 10 mm and length of 10 mm and printed at an 80 s/layer exposure with varying concentrations of BOC_2O , and varying layer heights (Figure 6). Compressive loading was performed at constant strain rate of 3 mm/min and load cell sampling frequency of 5 Hz. While all tests were performed with a similar strain rate and sampling frequency, we anticipate similar resultant properties at low strain rate due to the relatively low change in relaxation modulus of pHEMA with respect to time $(5-10\% \Delta E$ with a

time constant of roughly 500 s for unconfined compression).³³ We anticipate similar values of viscoelastic creep as a percentage difference in modulus in the expanded and unexpanded states so long as the absorption of water is negligible. However, if the pHEMA polymer does absorb water, we expect this value to increase dramatically.

After heating, samples that did not appreciably expand (50 um layer height and 0 wt % BOC₂O samples) increased in mechanical stiffness. We hypothesize that this is due to thermal curing, initiating any unreacted monomer and driving the degree of conversion close to 100% (Figure 6A,B). Samples that did expand experienced a drastic shift in mechanical properties, with both stiffness and density decreasing dramatically (Figure 6A–C). In the case of 150 μ m/10 wt % BOC₂O samples, the density became comparable with that of commercial Styrofoam³² (shown in red dotted lines, Figure 6D). Open-cell foams that did not expand only decreased in density slightly. Overall, while the expanded pHEMA resin is not as stiff or as strong as Styrofoam, it may be advantageous for some applications where destructibility is desired, such as in a cushioning foam. During compressive testing, we found that samples exhibited a short range of elastic deformation followed by a large region of plastic deformation. We anticipate the effect of residual stresses to be negligible after expansion due to the low glass transition temperature of pHEMA (~100 °C) and the length of time the pieces are held above their glass transition temperature, after which we expect all residual stresses from expansion to normalize.

Technology Demonstration. Two applications for the foaming resin were explored: an expanding raft for cargo transport and an expanding airfoil for electricity generation (these can be seen in the supplemental videos). In the former, a structural boat hull was printed from a resin composition consisting of HEMA containing 10 wt % BOC2O at 1× scale (8.6 cm in length) and was floated in a tank of water. Weights were added to the floating boat until 12.7 g of mass was added, at which point it sank. The boat hull was then placed in an oven at 200 °C for 10 min to initiate expansion, and the test was repeated with the boat hull now being 28.6 cm in length. In the second test, the boat could carry over 250 g of mass and returned to the surface (due to the trapped gases within the foam structure) even when forcefully submerged. In the second application, a helical air turbine was designed and printed at 1× scale (3.6 cm in diameter) and was placed in front of a small fan blowing cold air at a distance of 15 cm. The helical turbine was mechanically connected via a pulley to a small DC electric generator, and the fan was turned on. The small turbine was not able to generate sufficient torque to spin the generator in the air stream. The helical turbine was then placed in an oven at 200 °C for 10 min and allowed to expand, and the test was repeated with the turbine now being 10.9 cm in diameter. In the second test, when exposed to the same conditions, the turbine generated sufficient torque to spin the generator and generate a small voltage (roughly 100 mV with no load).

CONCLUSION

We have demonstrated the facile formulation, chemical stability, printability, controllable expansion, controllable cell structure, and selected applications for a novel, highly expandable foam material made from 2-hydroxyethyl methacrylate (HEMA) and a blowing agent, di-tert-butyl dicarbonate (BOC₂O). We have demonstrated volumetric

expansion ratios up to 4000% by volume, surpassing the state of the art by 2 orders of magnitude. The highly expandable foam developed in this work allows for the production of large objects using small amounts of precursor resin, allowing for the fabrication of structures that are significantly larger than the build volume of the printer that produced them and are light enough to serve as airfoils or buoyancy aids. We believe that the capability to produce such large objects from a small printer with reasonable fidelity represents a significant advancement in the design space for 3D printing and a versatile tool for the future of manufacturing.

ASSOCIATED CONTENT

Solution Supporting Information

The Supporting Information is available free of charge at https://pubs.acs.org/doi/10.1021/acsami.0c02683.

Chemicals and sources, equipment, instrumentation, description of applied technology demonstrations, resin composition tables, NMR analysis, TGA results, GC–MS results, photographs of printing apparatus and bulk resin expansion (PDF)

Videos of printed part expansion (ZIP)

AUTHOR INFORMATION

Corresponding Author

Jonathan K. Pokorski — Department of NanoEngineering, University of California San Diego, Jacobs School of Engineering, La Jolla, California 92093, United States; orcid.org/0000-0001-5869-6942; Phone: 858-246-3183; Email: jpokorski@ucsd.edu

Authors

David M. Wirth — Department of NanoEngineering, University of California San Diego, Jacobs School of Engineering, La Jolla, California 92093, United States; orcid.org/0000-0003-0383-7626

Anna Jaquez — Department of NanoEngineering, University of California San Diego, Jacobs School of Engineering, La Jolla, California 92093, United States

Sofia Gandarilla — Department of NanoEngineering, University of California San Diego, Jacobs School of Engineering, La Jolla, California 92093, United States

Justin D. Hochberg – Department of NanoEngineering, University of California San Diego, Jacobs School of Engineering, La Jolla, California 92093, United States

Derek C. Church – Department of NanoEngineering, University of California San Diego, Jacobs School of Engineering, La Jolla, California 92093, United States

Complete contact information is available at: https://pubs.acs.org/10.1021/acsami.0c02683

Note

The authors declare no competing financial interest.

ACKNOWLEDGMENTS

D.M.W., J.D.H, and J.K.P. acknowledge funding from the National Science Foundation (OISE 1844463). A.J. and S.G. would like to thank the ENLACE program at UCSD for research support.

REFERENCES

- (1) Ligon, S. C.; Liska, R.; Stampfl, J.; Gurr, M.; Mülhaupt, R. Polymers for 3D Printing and Customized Additive Manufacturing. *Chem. Rev.* **2017**, *117* (15), 10212–10290.
- (2) Ngo, T. D.; Kashani, A.; Imbalzano, G.; Nguyen, K. T. Q.; Hui, D. Additive Manufacturing (3D Printing): A Review of Materials, Methods, Applications and Challenges. *Composites, Part B* **2018**, *143*, 172–196
- (3) Liu, Y.; Campbell, J. H.; Stein, O.; Jiang, L.; Hund, J.; Lu, Y. Deformation Behavior of Foam Laser Targets Fabricated by Two-Photon Polymerization. *Nanomaterials* **2018**, *8* (7), 498.
- (4) Xiong, W.; Liu, Y.; Jiang, L. J.; Zhou, Y. S.; Li, D. W.; Jiang, L.; Silvain, J.-F.; Lu, Y. F. Laser-Directed Assembly of Aligned Carbon Nanotubes in Three Dimensions for Multifunctional Device Fabrication. *Adv. Mater.* **2016**, 28 (10), 2002–2009.
- (5) Chen, L.; Wu, Q.; Wei, G.; Liu, R.; Li, Z. Highly Stable Thiol—Ene Systems: From Their Structure—Property Relationship to DLP 3D Printing. J. Mater. Chem. C 2018, 6 (43), 11561–11568.
- (6) Zhang, G.; Wang, B.; Ma, L.; Wu, L.; Pan, S.; Yang, J. Energy Absorption and Low Velocity Impact Response of Polyurethane Foam Filled Pyramidal Lattice Core Sandwich Panels. *Compos. Struct.* **2014**, *108*, 304–310.
- (7) https://www.grandviewresearch.com/industry-analysis/polymer-foam-market (accessed Oct 7, 2019).
- (8) Chen, Q.; Cao, P.-F.; Advincula, R. C. Mechanically Robust, Ultraelastic Hierarchical Foam with Tunable Properties via 3D Printing. Adv. Funct. Mater. 2018, 28 (21), 1800631.
- (9) Chen, Q.; Zhao, J.; Ren, J.; Rong, L.; Cao, P.-F.; Advincula, R. C. 3D Printed Multifunctional, Hyperelastic Silicone Rubber Foam. *Adv. Funct. Mater.* **2019**, 29 (23), 1900469.
- (10) Singh, A. K.; Patil, B.; Hoffmann, N.; Saltonstall, B.; Doddamani, M.; Gupta, N. Additive Manufacturing of Syntactic Foams: Part 1: Development, Properties, and Recycling Potential of Filaments. *JOM* **2018**, *70* (3), 303–309.
- (11) Marascio, M. G. M.; Antons, J.; Pioletti, D. P.; Bourban, P.-E. 3D Printing of Polymers with Hierarchical Continuous Porosity. *Adv. Mater. Technol.* **2017**, 2 (11), 1700145.
- (12) Visser, C. W.; Amato, D. N.; Mueller, J.; Lewis, J. A. Architected Polymer Foams via Direct Bubble Writing. *Adv. Mater.* **2019**, 31 (46), 1904668.
- (13) Song, X.; Zhang, Z.; Chen, Z.; Chen, Y. Porous Structure Fabrication Using a Stereolithography-Based Sugar Foaming Method. J. Manuf. Sci. Eng. 2017, 139 (3), 031015.
- (14) Wagner, A.; Kreuzer, A. M.; Göpperl, L.; Schranzhofer, L.; Paulik, C. Foamable Acrylic Based Ink for the Production of Light Weight Parts by Inkjet-Based 3D Printing. *Eur. Polym. J.* **2019**, *115*, 325–334
- (15) Carve, M.; Włodkowic, D. 3D-Printed Chips: Compatibility of Additive Manufacturing Photopolymeric Substrata with Biological Applications. *Micromachines* **2018**, *9* (2), 91.
- (16) Ashby, M. Materials Selection in Mechanical Design, 3rd ed.; Elsevier, 2005.
- (17) Jing, C.; Suzuki, Y.; Matsumoto, A. Thermal Decomposition of Methacrylate Polymers Containing Tert-Butoxycarbonyl Moiety. *Polym. Degrad. Stab.* **2019**, *166*, 145–154.
- (18) Kotz, F.; Arnold, K.; Bauer, W.; Schild, D.; Keller, N.; Sachsenheimer, K.; Nargang, T. M.; Richter, C.; Helmer, D.; Rapp, B. E. Three-Dimensional Printing of Transparent Fused Silica Glass. *Nature* **2017**, *544* (7650), 337–339.
- (19) Thrasher, C. J.; Schwartz, J. J.; Boydston, A. J. Modular Elastomer Photoresins for Digital Light Processing Additive Manufacturing. ACS Appl. Mater. Interfaces 2017, 9 (45), 39708–30716
- (20) Roorda, W. E.; Bouwstra, J. A.; de Vries, M. A.; Junginger, H. E. Thermal Behavior of Poly Hydroxy Ethyl Methacrylate (PHEMA) Hydrogels. *Pharm. Res.* **1988**, 5 (11), 722–725.
- (21) Wu, J.; Zhao, Z.; Hamel, C. M.; Mu, X.; Kuang, X.; Guo, Z.; Qi, H. J. Evolution of Material Properties during Free Radical Photopolymerization. *J. Mech. Phys. Solids* **2018**, *112*, 25–49.

- (22) Stehr, J. Chemical Blowing Agents in the Rubber Industry. Past Present and Future? *Int. Polym. Sci. Technol.* **2016**, 43 (5), 1–10.
- (23) Sadik, T.; Pillon, C.; Carrot, C.; Reglero Ruiz, J.-A. Dsc Studies on the Decomposition of Chemical Blowing Agents Based on Citric Acid and Sodium Bicarbonate. *Thermochim. Acta* **2018**, 659, 74–81.
- (24) Williams, J. M.; Wrobleski, D. A. Microstructures and Properties of Some Microcellular Foams. *J. Mater. Sci.* **1989**, 24 (11), 4062–4067.
- (25) Wypych, G. Handbook of Foaming and Blowing Agents, 1st ed.; ChemTec Publishing, 2017.
- (26) Meakin, J. R.; Hukins, D. W. L.; Aspden, R. M.; Imrie, C. T. Rheological Properties of Poly(2-Hydroxyethyl Methacrylate) (PHEMA) as a Function of Water Content and Deformation Frequency. *J. Mater. Sci.: Mater. Med.* **2003**, *14* (9), 783–787.
- (27) Celina, M. Method for Epoxy Foam Production Using a Liquid Anhydride. US 8193256B1, June 5, 2012.
- (28) Iseki, M.; Hiraoka, Y.; Jing, C.; Okamura, H.; Sato, E.; Matsumoto, A. Effect of Glass Transition Temperature on Heat-Responsive Gas Bubbles Formation from Polymers Containing Tert-Butoxycarbonyl Moiety. J. Appl. Polym. Sci. 2018, 135 (19), 46252.
- (29) Dean, C. S.; Tarbell, D. S.; Friederang, A. W. Synthesis and Kinetics of Decomposition of Di-Tert-Butyl Tricarbonate, Di-Tert-Butyl Dithioltricarbonate, and the Related Dicarbonates. *J. Org. Chem.* **1970**, 35 (10), 3393–3397.
- (30) Greenberg, A. R.; Kusy, R. P. Influence of Crosslinking on the Glass Transition of Poly(Acrylic Acid). *J. Appl. Polym. Sci.* **1980**, 25 (8), 1785–1788.
- (31) Walley, S. M.; Field, J. E. Strain Rate Sensitivity of Polymers in Compression from Low to High Rates. *DYMAT J.* **1994**, *1*, 211–227.
- (32) Di Landro, L.; Sala, G.; Olivieri, D. Deformation Mechanisms and Energy Absorption of Polystyrene Foams for Protective Helmets. *Polym. Test.* **2002**, *21* (2), 217–228.
- (33) Kaufman, J. D.; Miller, G. J.; Morgan, E. F.; Klapperich, C. M. Time-Dependent Mechanical Characterization of Poly(2-Hydroxyethyl Methacrylate) Hydrogels Using Nanoindentation and Unconfined Compression. *J. Mater. Res.* **2008**, 23 (5), 1472–1481.